Polymer Journal (2015) 47, 513–521

www.nature.com/pj

ORIGINAL ARTICLE

Synthesis of 1,3,4-thiadiazole-based donor–acceptor alternating copolymers for polymer solar cells with high open-circuit voltage

Seijiro Fukuta[1,2], Zhongqiang Wang[3], Satoshi Miyane[1,2], Tomoyuki Koganezawa[4], Takeshi Sano[5], Junji Kido[3], Hideharu Mori[1,3], Mitsuru Ueda[6] and Tomoya Higashihara[1,2,7]

We report the synthesis and characterization of novel 1,3,4-thiadiazole (TDz)-containing π-conjugated alternating copolymers with donor units, such as thiophene (PTDzTh), selenophene (PTDzSe), thieno[3,4-*b*]thiophene (PTDzTT), 3,3′-didodecyl-2,2′-bithiophene (PTDzBTh) and (*E*)-1,2-di-(3-dodecylthiophene)vinylene (PTDzTV). The TDz-containing polymers show deep highest occupied molecular orbital (HOMO) energy levels at approximately − 5.50 to − 5.20 eV due to the electron deficiency of the TDz unit. In addition, PTDzTV shows a relatively extended absorption wavelength (λ_{onset} = 629 nm). The microstructures of the film state are primarily influenced by the interdigitation of the side chains, and PTDzTT with a rigid backbone forms a densely packed crystalline structure, as evidenced by grazing incident wide-angle X-ray scattering experiments. Polymer solar cells using the TDz polymers showed high open-circuit voltages up to 0.965 V based on the deep HOMO energy levels, and PTDzTV showed the highest power conversion efficiency of 0.529% among the polymers.
Polymer Journal (2015) **47,** 513–521; doi:10.1038/pj.2015.19; published online 22 April 2015

INTRODUCTION

In recent decades, small π-conjugated organic molecules or polymers have received substantial attention due to their semiconducting nature and processability, enabling printable electronic devices, such as organic light-emitting diodes, organic thin-film transistors and organic photovoltaics.[1–3] Among organic photovoltaics, polymer solar cells (PSCs) are one of the applications of π-conjugated polymers, and they use a blended film of a p-type semiconducting polymer and an n-type fullerene derivative as a photoelectric conversion layer.[4] For example, a combination of regioregular poly(3-hexylthiophene) and [6,6]-phenyl-C_{61}-butyric acid methyl ester is commonly used as the photoactive layer of a PSC, called a bulk-heterojunction system, showing a 3–5% power conversion efficiency (PCE).[5–7] Recently, the PCE has been dramatically improved to 10% by the development of p-type semiconducting polymers having an extended absorption wavelength.[8] This breakthrough is attributed to the development of a strategy in molecular design, which is the donor–acceptor alternative structure.[9–11] The copolymerization of electron-rich (donor) and electron-deficient (acceptor) units enables tuning of the energy levels of the high occupied molecular orbital (HOMO) and the low unoccupied molecular orbital (LUMO) of the π-conjugated polymer. Therefore, when this polymer is applied to a PSC, a high built-in potential and a LUMO offset between the p-type and n-type materials should be achieved, maintaining an extended absorption wavelength to afford a high PCE.[12]

1,3,4-Thiadiazole (TDz) is a promising candidate as an electron-deficient unit having two electron-withdrawing imine (C = N) groups. In addition, TDz is a small unit compared with thiophene because of the lack of hydrogen atoms at the 3- and 4-positions.[13–18] The compact structure provides a great advantage in suppressing the torsion of the polymer backbone and interchain steric hindrance, achieving a high PCE in the PSC device due to the high hole mobility of the polymer and the low contact resistance at the polymer/electrode interface. We previously reported that the TDz-containing polymer poly[2,5-thiophene-alt-5′,5′-(2′′,5′′-bis(3′,4′-dihexylthien-2′-yl)-1′′,3′′,4′′-thiadiazole)] (**P1**, Figure 1a) showed a high hole mobility ($8.81 \times 10^{-2}\,cm^{-2}\,V^{-1}\,s^{-1}$) in an organic thin-film transistor device.[17] By using a grazing incident wide-angle X-ray scattering (GIWAXS) measurement, it was demonstrated that **P1** formed densely stacked crystalline domains with a short π-π stacking distance (3.51 Å), and the π-plane of the polymers lies parallel to the substrate (face-on orientation).[19] Considering the relationship between the PSC performance and the microstructure of **P1**, the simple structure of a TDz unit is beneficial for improving PSC performance. In addition, several

[1]Department of Polymer Science and Engineering, Graduate School of Science and Engineering, Yamagata University, Yonezawa, Japan; [2]Innovative Flex Course for Frontier Organic Material Systems, Graduate School of Science and Engineering, Yamagata University, Yonezawa, Japan; [3]Department of Organic Device Engineering, Graduate School of Science and Engineering, and Research Center for Organic Electronics (ROEL), Yamagata University, Yonezawa, Yamagata, Japan; [4]Japan Synchrotron Radiation Research Institute, Sayo-gun, Hyogo, Japan; [5]Innovation Center for Organic Electronics (INOEL), Yamagata University, Yonezawa, Yamagata, Japan; [6]Department of Chemistry, Kanagawa University, Yokohama-shi, Kanagawa, Japan and [7]Japan Science and Technology Agency (JST), PRESTO, Kawaguchi, Saitama, Japan
Correspondence: Professor T Higashihara, Department of Polymer Science and Engineering, Graduate School of Science and Engineering, Yamagata University, 4-3-16 Jyonan, Yonezawa, Yamagata 992-8510, Japan.
E-mail: thigashihara@yz.yamagata-u.ac.jp
Received 18 January 2015; revised 19 February 2015; accepted 22 February 2015; published online 22 April 2015

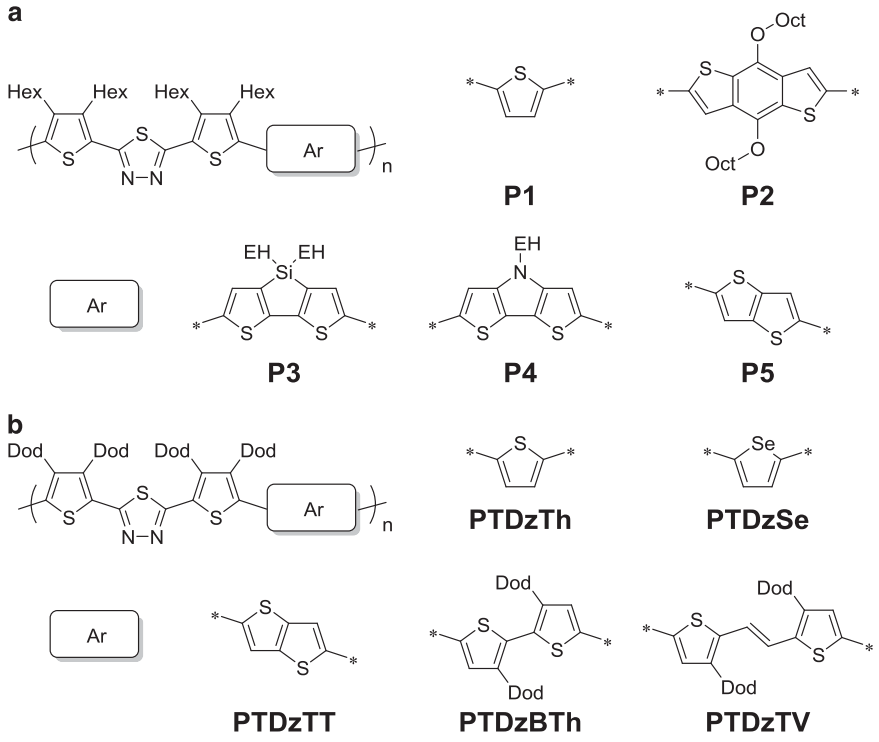

Figure 1 Chemical structures of TDz-containing polymers described in (**a**) previous reports and (**b**) this study.

TDz-containing polymers consisting of different donor units, such as benzodithiophene (**P2**), dithienosilole (**P3**), dithienopyrrole (**P4**) and thieno[3,4-*b*]thiophene (**P5**) were synthesized and applied to PSC devices (Figure 1a).[18] The best performance was achieved in a PSC using **P5** with 2.8% PCE, whereas other polymers provide substantially lower PCEs (<1%) due to low short-circuit current densities (J_{sc}s) and fill factors (*FF*s). The GIWAXS measurement revealed that the π-π stacking distance ($d_{\pi\text{-}\pi}$) is a dominant factor for PCE, and a compact donor unit provides a lower $d_{\pi\text{-}\pi}$ than a bulky donor containing a fused ring, such as benzodithiophene and dithienopyrrole.[19]

Based on these findings, in this study, we report the synthesis, the thermal and optoelectronic properties, as well as the morphology of a wide variety of new TDz-containing polymers with thiophene-based donor units, such as thiophene (PTDzTh), selenophene (PTDzSe), thieno[3,4-*b*]thiophene (PTDzTT), 3,3′-didodecyl-2,2′-bithiophene (PTDzBTh) and (*E*)-1,2-di-(3-dodecylthiophene)vinylene (PTDzTV), as depicted in Figure 1b, to clarify the relationships among the chemical structures, properties and crystalline morphology. Concerning their rigid structures, the solubilizing groups are extended from *n*-hexyl to *n*-dodecyl groups, causing a smaller increase in $d_{\pi\text{-}\pi}$ than that of branched alkyl side chains.[20,21]

MATERIALS AND METHODS

Materials

All of the reagents were used as received unless otherwise stated. Tetrahydrofuran (99.5%, Wako Chemicals Co., Ltd) was refluxed over sodium benzophenone under nitrogen for 2 h and then distilled immediately before use. 2,5-Bis(trimethylstannyl)thiophene was recrystallized before use. 3,4-Didodecylthiophene,[22] 2,5-bis(trimethylstannyl)selenophene,[23] 2,5-bis (trimethylstannyl)thieno[3,2-*b*]thiophene,[24] 5,5′-bis(trimethylstannyl)-3,3′-didodecyl-2,2′-bithiophene[25] and (*E*)-1,2-di(3-dodecyl-5-trimethylstannylthiophene)vinylene[26] were synthesized according to previously described methods.

Synthesis

3,4-Didodecyl-2-thiophenecarboxylic acid (2). To a tetrahydrofuran solution (60 ml) of 3,4-didodecylthiophene (**1**; 8.71 g, 20.7 mmol) a ^{n}BuLi solution (Kanto Chemical Co., Inc., Tokyo, Japan) in hexane (2.67 M × 8.54 ml = 22.8-mmol) was added dropwise at 0 °C. The solution was then stirred at room temperature for 1 h. After cooling the solution to 0 °C, CO_2 was bubbled through the reaction mixture for 2 h. The solution was warmed to room temperature followed by quenching with water, and the product was extracted with ether. The ether solution was neutralized with HCl(aq) and then washed with water and brine. After the solution was dried over $MgSO_4$ and filtered, the filtrate was evaporated under reduced pressure. The crude product was purified by flash silica gel column chromatography using hexane/ethyl acetate (9/1, v/v) as an eluent to afford **2** as a white solid (6.16 g, 64%). ^{1}H nuclear magnetic resonance (NMR) (400 MHz, $CDCl_3$, δ, p.p.m., 25 °C): 7.17 (s, 1H), 2.92 (t, 2H), 2.52 (t, 2H), 1.19 – 1.63 (m, 40H), 0.88 (t, 6H). ^{13}C NMR (100 MHz, $CDCl_3$, δ, p.p.m., 25 °C): 168.3, 152.0, 144.4, 127.7, 126.2, 32.0, 30.4, 30.0, 29.9, 29.8, 29.7, 29.6, 29.5, 28.8, 27.9, 22.8, 14.2. IR, ν (cm^{-1}): 1651 (C = O stretching), 1464 (C – O – H bending), 1286 (C – O stretching). Anal. Calcd. for $C_{29}H_{52}O_2S$ (%): C, 74.94, H, 11.28. Found (%): C, 74.37, H, 11.83.

N,N′-Bis(3,4-didodecylthien-2-ylcarbonyl)hydrazine (3). To a dry *N*-methylpyrrolidone solution (20 ml) of **2** (4.00 g, 8.65 mmol) was added dropwise at 0 °C thionyl chloride (0.652 ml, 9.01 mmol). The solution was then stirred at room temperature for 1.5 h. Triethylamine (1.30 ml, 12.9 mmol) and hydrazine anhydrous (0.136 ml, 4.29 mmol) were added and stirred overnight at 50 °C. The reaction was quenched with water, and the product was extracted with ether. The combined organic layer was washed with water and brine. After the solution was dried over $MgSO_4$ and filtered, the filtrate was evaporated under reduced pressure. The crude product was purified by flash silica gel column chromatography using hexane/ethyl acetate (9/1, v/v) as an eluent to afford **3** as a yellow solid (3.44 g, 86%). ^{1}H NMR (400 MHz, $CDCl_3$, δ, p.p.m., 25 °C): 8.49 (s, 2H), 7.02 (s, 2H), 2.88 (t, 4H), 2.52 (t, 4H), 1.19 – 1.66 (m, 80H), 0.90 (m, 12H). ^{13}C NMR (100 MHz, $CDCl_3$, δ, p.p.m., 25 °C): 160.7, 148.4, 144.4, 126.8, 123.1, 32.0, 30.7, 30.0, 29.8, 29.8, 29.7, 29.6, 29.5, 28.8, 28.1, 22.8, 14.2. IR, ν (cm^{-1}): 3175 (N – H stretching), 1586 (C = O stretching). MS *m/z*: Calcd. for $C_{58}H_{104}N_2Na_1O_2S_2$, 947.74, found 947.75.

*2,5-Bis(3′,4′-didodecylthien-2′-yl)-1,3,4-thiadiazole (**4**)*. A toluene solution (80 ml) of **3** (3.34 g, 3.61 mmol) and 2,4-bis(4-methoxyphenyl)-1,3,2,4-dithiadiphosphetane-2,4-dithione (Lawesson's reagent, 1.75 g, 4.33 mmol) was refluxed for 3 h. The resulting solution was extracted with $CHCl_3$, and the organic phase was washed with NaOH(aq), water and brine. After the solution was dried over $MgSO_4$ and filtered, the filtrate was evaporated under reduced pressure. The filtrate was then purified by flash silica gel column chromatography using hexane/ethyl acetate (19/1, v/v) as an eluent to afford **4** as a yellow solid (2.08 g, 63%). ^{1}H NMR (400 MHz, $CDCl_3$, δ, p.p.m., 25 °C): 7.07 (s, 2H), 2.88 (t, 4H), 2.55 (t, 4H), 1.22 – 1.69 (m, 80H), 0.88 (m, 12H). ^{13}C NMR (100 MHz, $CDCl_3$, δ, p.p.m., 25 °C): 160.5, 143.5, 143.2, 127.1, 33.6, 33.5, 32.0, 30.2, 30.0, 29.7, 29.4, 29.1, 28.6, 28.5, 22.8, 14.1. IR, ν (cm^{-1}): 1548 (C = N stretching). MS *m/z*: Calcd. for $C_{58}H_{103}N_2S_3$, 923.73, found 923.73.

*2,5-Bis(5′-bromo-3′,4′-didodecylthien-2′-yl)-1,3,4-thiadiazole (**5**)*. To **4** (1.79 g, 1.94 mmol) in $CHCl_3$ (20 ml) *N*-bromosuccinimide (1.22 g, 6.79 mmol) was added, and the solution was stirred overnight. The reaction was quenched with water, and the product was extracted with ether. After the solution was dried over $MgSO_4$ and filtered, the filtrate was condensed under reduced pressure. The crude product was then purified by flash silica gel column chromatography using hexane/ethyl acetate (24/1, v/v) as an eluent to afford **5** as a yellow solid (1.92 g, 91%). ^{1}H NMR (400 MHz, $CDCl_3$, δ, p.p.m., 25 °C): 2.85 (t, 4H), 2.57 (t, 4H), 1.19 – 1.59 (m, 80H), 0.88 (m, 12H). ^{13}C NMR (100 MHz, $CDCl_3$, δ, p.p.m., 25 °C): 159.1, 143.4, 143.1, 127.4, 114.5, 32.1, 30.2, 30.1, 29.8, 29.5, 29.1, 29.0, 28.6, 28.5, 22.8, 14.2. IR, ν (cm^{-1}): 1546 (C = N stretching). Calcd. for $C_{58}H_{100}N_2S_3$ (%): C, 64.42, H, 9.32, N, 2.59. Found (%): C, 64.49, H, 9.57, N, 2.38.

*Poly[2,5-thiophene-alt-5′,5′-(2′′,5′′-bis(3′,4′-didodecylthien-2′-yl)-1′′,3′′,4′′-thiadiazole)] (**PTDzTh**)*. To **5** (0.211 g, 0.195 mmol) and 2,5-bis(trimethylstannyl)thiophene (0.0799 g, 0.195 mmol) $Pd_2(dba)_3$ (10.2 mg, 0.0111 mmol) and tri(*o*-tolyl)phosphine (29.8 mg, 0.0979 mmol) in toluene (6.2 ml) in nitrogen was added, which was deoxygenated by bubbling with dry nitrogen for 15 min. The solution was refluxed for 2 days. 2-(Tributylstannyl)thiophene (0.013 ml, 0.039 mmol) was then added and stirred for 1 h. Subsequently, 2-bromothiophene (0.0057 ml, 0.059 mmol) was added and stirred for 1 h. After quenching the reaction with HCl(aq) and neutralizing with $NaHCO_3$(aq), the product was extracted with $CHCl_3$. The $CHCl_3$ solution was washed with KF(aq) and was condensed under reduced pressure. Next, the solution was passed through a silica gel column using $CHCl_3$ as an eluent and poured into water/methanol to precipitate the polymer. The polymer was purified by Soxhlet extraction using methanol, acetone, acetone/hexane (1/1, v/v) and $CHCl_3$. After evaporating the $CHCl_3$ solution, the polymer was freeze dried from its absolute benzene solution to afford PTDzTh as a red solid (0.128 g, 65%). Size exclusion chromatography (SEC): molecular weight (M_n) = 26 600 g mol^{-1}, dispersity ($Đ$) = 1.77. ^{1}H NMR (400 MHz, $CDCl_3$, δ, p.p.m., 25 °C): 7.23 (s, 2H), 2.91 (s, 4H), 2.80 (s, 4H), 1.21 – 1.70 (m, 80H), 0.87 (t, 12H). IR, ν (cm^{-1}): 1551 (C = N stretching). Anal. Calcd. for $C_{62}H_{104}N_2S_3$ (%): C, 74.04, H, 10.42, N, 2.69, S, 12.75. Found (%): C, 73.76, H, 10.15, N, 2.68, S, 12.72.

*Poly[2,5-selenophene-alt-5′,5′-(2′′,5′′-bis(3′,4′-didodecylthien-2′-yl)-1′′,3′′,4′′-thiadiazole)] (**PTDzSe**)*. To **5** (0.200 g, 0.185 mmol) and 2,5-bis(trimethylstannyl)selenophene (0.0846 g, 0.182 mmol) $Pd_2(dba)_3$ (10.9 mg, 0.0119 mmol) and tri(o-tolyl)phosphine (60.0 mg, 0.197 mmol) in toluene (8.0 ml) in nitrogen was added, which was deoxygenated by bubbling with dry nitrogen for 15 min. The solution was refluxed for 2 days. 2-(Tributylstannyl)thiophene (0.012 ml, 0.037 mmol) was then added and stirred for 1 h. Subsequently, 2-bromothiophene (0.0054 ml, 0.056 mmol) was added and stirred for 1 h. After quenching the reaction with HCl(aq) and neutralizing with $NaHCO_3$(aq), the product was extracted with $CHCl_3$. The $CHCl_3$ solution was washed with KF (aq) and was condensed under reduced pressure. Then, the solution was passed through a silica gel column using $CHCl_3$ as an eluent and poured into water/methanol to precipitate the polymer. The polymer was purified by Soxhlet extraction using methanol and $CHCl_3$. After evaporating the $CHCl_3$ solution, the polymer was freeze dried from its absolute benzene solution to afford PTDzSe as a red solid (0.134 g, 72%). SEC: M_n = 17 800 g mol^{-1}, $Đ$ = 2.10. 1H NMR (400 MHz, $CDCl_3$, δ, p.p.m., 25 °C): 7.39 (s, 2H), 2.91 (s, 4H), 2.77 (s, 4H), 1.68–1.20 (m, 80H), 0.88 (t, 12H). IR, ν (cm^{-1}): 1550 (C = N stretching). Anal. Calcd. for $C_{62}H_{104}N_2S_3Se$ (%): C, 70.74, H, 9.96, N, 2.66. Found (%): C, 70.75, H, 9.96, N, 2.57.

*Poly[2,5-thieno[3,2-b]thiophene-alt-5′,5′-(2′′,5′′-bis(3′,4′-didodecylthien-2′-yl)-1′′,3′′,4′′-thiadiazole)] (**PTDzTT**)*. To **5** (0.206 g, 0.191 mmol) and 2,5-bis (trimethylstannyl)thieno[3,2-*b*]thiophene (0.0890 g, 0.191 mmol) $Pd_2(dba)_3$ (11.8 mg, 0.0129 mmol) and tri(o-tolyl)phosphine (35.4 mg, 0.0955 mmol) in toluene (6.2 ml) in nitrogen was added, which was deoxygenated by bubbling with dry nitrogen for 15 min. The solution was refluxed for 2 days. 2-(Tributylstannyl)thiophene (0.012 ml, 0.037 mmol) was then added and stirred for 1 h. Then, 2-bromothiophene (0.0055 ml, 0.057 mmol) was added and stirred for 1 h. After quenching the reaction with HCl(aq) and neutralizing with $NaHCO_3$(aq), the product was extracted with $CHCl_3$ and *o*-dichlorobenzene (*o*-DCB). The $CHCl_3$ and *o*-DCB solution was washed with KF(aq) and was condensed under reduced pressure. Next, the solution was passed through a silica gel column using $CHCl_3$ as an eluent and poured into water/methanol to precipitate the polymer. The polymer was purified by Soxhlet extraction using methanol, acetone, hexane and $CHCl_3$. After evaporating the $CHCl_3$ solution, the polymer was freeze dried from its absolute benzene solution to afford PTDzTT as a red solid (0.155 g, 75%). SEC: M_n = 21 100 g mol^{-1}, $Đ$ = 1.78. ^{1}H NMR (400 MHz, $CDCl_3$, δ, p.p.m., 25 °C): 7.39 (s, 2H), 2.93 (s, 4H), 2.81 (s, 4H), 1.68–1.21 (m, 80H), 0.87 (t, 12H). IR, ν (cm^{-1}): 1543 (C = N stretching). Anal. Calcd. for $C_{64}H_{104}N_2S_5$ (%): C, 72.39, H, 9.87, N, 2.64, S, 15.10. Found (%): C, 72.30, H, 9.59, N, 2.52, S, 15.40.

*Poly[5,5′-(3,3′-didodecyl-2,2′-bithiophene)-alt-5′′,5′′-(2′′′,5′′′-bis(3′′,4′′-didodecylthien-2′′-yl)-1′′′,3′′′,4′′′-thiadiazole)] (**PTDzBTh**)*. To **5** (0.200 g, 0.185 mmol) and 5,5′-bis(trimethylstannyl)-3,3′-didodecyl-2,2′-bithiophene (0.153 g, 0.185 mmol) $Pd_2(dba)_3$ (12.2 mg, 0.0133 mmol) and tri(o-tolyl)phosphine (38.6 mg, 0.127 mmol) in toluene (6.2 ml) in nitrogen was added, which was deoxygenated by bubbling with dry nitrogen for 15 min. The solution was refluxed for 2 days. 2-(Tributylstannyl)thiophene (0.012 ml, 0.037 mmol) was added and stirred for 1 h. Subsequently, 2-bromothiophene (0.0054 ml, 0.056 mmol) was added and stirred for 1 h. After quenching the reaction with HCl(aq) and neutralizing with $NaHCO_3$(aq), the product was extracted with $CHCl_3$. The $CHCl_3$ solution was washed with KF(aq) and was condensed under reduced pressure. Then, the solution was passed through a silica gel column using $CHCl_3$ as an eluent and poured into water/methanol to precipitate the polymer. The polymer was purified by Soxhlet extraction using methanol, acetone, acetone/hexane (1/1, v/v) and $CHCl_3$. After evaporating $CHCl_3$, the polymer was freeze dried from its absolute benzene solution to afford PTDzBTh as a red solid (0.105 g, 39%). SEC: M_n = 27 400 g mol^{-1}, $Đ$ = 1.51. ^{1}H NMR (400 MHz, $CDCl_3$, δ, p.p.m., 25 °C): 7.13 (s, 2H), 2.91 (s, 4H), 2.78 (s, 4H), 2.59 (s, 4H), 1.68–1.20 (m, 120H), 1.10–0.82 (m, 18H). IR, ν (cm^{-1}): 1518 (C = N stretching). Anal. Calcd for $C_{90}H_{154}N_2S_5$ (%): C, 75.88, H, 10.90, N, 1.97, S, 11.25. Found (%): C, 75.97, H, 11.42, N, 1.88, S, 11.59.

*Poly[5,5′-((E)-1,2-di(3-dodecylthiophene)vinylene)-alt-5′′,5′′-(2′′′,5′′′-bis(3′′,4′′-didodecylthien-2′′-yl)-1′′′,3′′′,4′′′-thiadiazole)] (**PTDzTV**)*. To **5** (0.201 g, 0.186 mmol) and (*E*)-1,2-di(3-dodecyl-5-trimethylstannylthiophene)vinylene (0.159 g, 0.186 mmol) $Pd_2(dba)_3$ (12.0 mg, 0.0131 mmol) and tri(o-tolyl) phosphine (29.9 mg, 0.0982 mmol) in toluene (7.0 ml) in nitrogen was added, which was deoxygenated by bubbling with dry nitrogen for 15 min. The solution was refluxed for 2 days. 2-(Tributylstannyl)thiophene (0.012 ml, 0.037 mmol) was then added and stirred for 1 h. Next, 2-bromothiophene (0.0054 ml, 0.056 mmol) was added and stirred for 1 h. Subsequently, the solution was poured into water/methanol to precipitate the polymer. The polymer was purified by Soxhlet extraction using methanol, acetone, hexane and $CHCl_3$. After evaporating $CHCl_3$, the polymer was poured into methanol to afford PTDzTV as a purple solid (0.150 g, 55%). SEC: M_n = 26 600 g mol^{-1}, $Đ$ = 1.64. ^{1}H NMR (400 MHz, $CDCl_3$, δ, p.p.m., 25 °C): 7.01 (s, 2H), 7.00 (s, 2H), 2.90 (s, 4H), 2.79 (s, 4H), 2.68 (s,4H), 1.72–1.19 (m, 130H), 0.97–0.81 (m, 18H). IR, ν (cm^{-1}): 1531 (C = N stretching). Anal. Calcd. for $C_{92}H_{156}N_2S_5$ (%): C, 76.18, H, 10.84, N, 1.93, S, 11.05. Found (%): C, 76.55, H, 11.18, N, 1.76, S, 10.60.

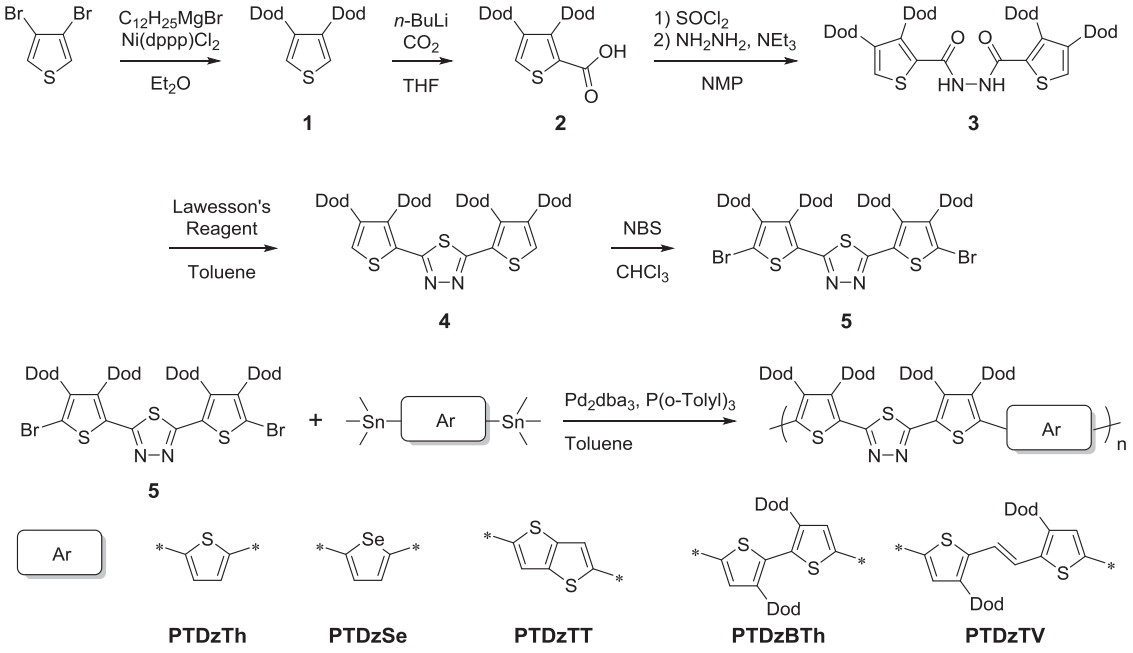

Scheme 1 Synthetic routes for PTDzTh, PTDzSe, PTDzTT, PTDzBTh and PTDzTV.

Measurements

Molecular weights and *Đ* were measured by SEC on a (Jasco GULLIVER 1500, Jasco, Co., Tokyo, Japan) equipped with a pump, an absorbance detector (ultraviolet (UV), $\lambda = 254$ nm) and three polystyrene gel columns based on a conventional calibration curve using polystyrene standards. $CHCl_3$ (40 °C) was used as a carrier solvent at a flow rate of 1.0 ml min^{-1}. ^{1}H and ^{13}C NMR spectra were recorded on a JEOL JNM-ECX400 (JEOL, Ltd., Tokyo, Japan) in chloroform-*d* calibrated to tetramethylsilane as an internal standard (δH 0.00). Fourier-transform infrared spectroscopy (FT-IR) spectra were obtained on a Horiba FT-720 spectrometer (Horiba, Ltd., Kyoto, Japan). Thermal analysis was performed on a Seiko EXSTAR 6000 TG/DTA 6300 thermal analyzer (Seiko Instruments Inc., Chiba, Japan) at a heating rate of 10 °C min^{-1} for thermogravimetry, and differential scanning calorimetry (DSC) was performed on Seiko DSC 6300 (Seiko Instruments Inc.) connected to a cooling system at a heating rate of 10 °C min^{-1}. UV–visible absorption spectra were recorded using a Hitachi U-4100 spectrophotometer (Hitachi High-Tech Science Co., Tokyo, Japan). For the thin-film spectra, polymers were dissolved in $CHCl_3$ and then filtered through a 0.45-μm pore size polytetrafluoroethylene (PTFE) membrane syringe filter, followed by drop casting onto a quartz substrate. HOMO and LUMO levels in the solid films were recorded by a Riken Keiki AC-3 photoelectron yield spectrometer (Riken Keiki Co., Ltd., Tokyo, Japan), and the UV–visible absorption edge was obtained from the absorption spectra of the films. GIWAXS measurements were conducted at beamline BL46XU of SPring-8, Hyogo, Japan. The sample films were prepared by drop casting the polymer solutions (10 mg ml^{-1} in $CHCl_3$) on the Si substrates, followed by air drying for 1 h. The samples were irradiated at a fixed incident angle on the order of 0.12° through a Huber diffractometer (HUBER Diffraktionstechnik GmbH & Co. KG, Rimsting, Germany) with an X-ray energy of 12.398 keV (X-ray wavelength, $\lambda = 0.10$ nm), and the GIWAXS patterns were recorded with a two-dimensional image detector (Pilatus 300 K, DECTRIS, Baden, Switzerland) with a sample-to-detector distance of 174 mm.

PSC fabrication and characterization

Chlorobenzene (CB) and [6,6]-phenyl C_{71}-butyric acid methyl ester ($PC_{71}BM$) were purchased from Sigma-Aldrich Co. LLC. (Tokyo, Japan) and Luminescence Technology Corporation (Hsin-Chu, Taiwan, R.O.C), respectively. Glass substrates coated with transparent indium tin oxide (ITO) with a sheet resistivity of 15 ohm sq^{-1} and patterned with discrete 3-mm stripes were purchased from Luminescence Technology Corporation. The pre-patterned ITO-coated substrates were cleaned with detergent, deionized water, acetone and isopropanol by sonication and then treated in UV–ozone for 30 min before coating the layers. For the cells with a sandwiched device structure, 40-nm PEDOT:PSS (poly (3,4-ethylenedioxythiophene):poly(styrenesulfonate)) (Baytron PVP AI 4083 (H.C. Starck Ltd., Tokyo, Japan)) was spin coated and annealed at 120 °C for 15 min on a hotplate in air. The PEDOT:PSS-coated substrates were transferred to a glove box, and the active layers of Polymer:$PC_{71}BM$ were spin coated from a solution of polymer:$PC_{71}BM$ (1:1 by weight) in CB. Calcium (Ca) and aluminum (Al) were subsequently deposited as a cathode using a shadow mask in the cells, which were thermally evaporated in a vacuum chamber with a base pressure of 1×10^{-6} Pa. The thicknesses and deposition rates were monitored by quartz crystal sensors. The active area of each cell was $\sim 3 \times 3$ mm^2, defined by the overlap of the ITO and Al. The fabricated cells were encapsulated in a nitrogen-filled glove box and then brought to ambient conditions for characterization of current density–voltage (*J-V*) using a CEP-2000 integrated system by Bunkoukeiki Co., Ltd, Tokyo, Japan. Light state *J-V* characteristics were measured under 100 mW cm^{-2} Air mass 1.5G (AM1.5G) simulated light.

RESULTS AND DISCUSSION

Synthesis of TDz-containing polymers

The general synthetic route to the electron-deficient monomers and polymers is displayed in Scheme 1. The TDz-containing monomer **5** was synthesized according to the same procedure as that in previous reports, except for the change from *n*-hexyl groups to *n*-dodecyl groups.[17] Dodecyl side chains are introduced into the polymers to improve the solubility because the previously reported polymer, **P5**, showed poor solubility, even in hot *o*-DCB. The polymers were synthesized by the Stille coupling polymerization between **5** and different distannyl compounds. After the Soxhlet extraction, all of the polymers with moderate molecular weights ($M_n = 17.8$–32.9 kg mol^{-1}) were obtained, which are summarized in Table 1. All of the polymers, except for PTDzTT, were successfully solubilized in tetrahydrofuran, $CHCl_3$, hot CB and hot *o*-DCB, whereas PTDzTT is soluble in these hot solvents.

Thermal properties

The thermal stability of the polymers was evaluated by TG/DTA (differential thermal analysis) measurements, and the data are summarized in Table 1. All of the polymers show nearly the same weight loss behavior with 5 wt% weight loss temperatures ($T_{d5\%}$) at ~400 °C (Figure 2a). This result indicates that all of the polymers have sufficient thermal stability for PSC fabrication. The DSC measurement revealed that the melting point (T_m) of PTDzTh, PTDzSe and PTDzTT is ~180 °C (Figures 2b and d). Compared with these values, the T_m values of PTDzBTh and PTDzTV are 90 and 154 °C (Figures 2e and f), respectively, are significantly lower due to the high content of dodecyl groups.

Optical and electronic properties

The UV–visible spectra of the as-cast polymer films are depicted in Figure 3. PTDzTh, PTDzSe and PTDzTT show an absorption maxima (λ_{max}) at 511–520 nm and an onset of absorption spectra (λ_{onset}) at 588–596 nm, which are nearly the same as those of **P1** (λ_{max} = 513 nm and λ_{onset} = 591 nm).[17] However, the λ_{max} of PTDzBTh (483 nm) is substantially shorter compared with the others, despite having a similar λ_{onset} (596 nm). This difference indicates that in the solid film state of PTDzBTh, most of the polymer backbones are twisted to reduce the conjugation length due to a steric hindrance induced by the head-to-head structure of 3,3′-didodecyl-2,2′-bithiophene.[25] This presumption is also supported by the absence of a shoulder peak attributed to an intermolecular packing structure. However, an approximate 30-nm red shift is found in the λ_{max} and λ_{onset} for PTDzTV (547 and 629 nm), which would be preferable for PSC application. Because the steric hindrance in the donor units is reduced by the introduction of a vinylene group, it appears that the optical band gap (E_g^{opt}) is effectively decreased due to the extended conjugation length of the thienylene vinylene unit.

Photoelectron yield spectroscopy was performed for the as-cast polymer films to investigate the HOMO energy levels. LUMO energy levels were estimated from the calculated HOMO values and the E_g^{opt}, according to the equation LUMO = HOMO+E_g^{opt}. As summarized in Figure 4, all of the polymers have significantly deeper HOMO energy levels than that of regioregular poly(3-hexylthiophene) due to the strong electron deficiency of the TDz units, which would provide high open-circuit voltage (V_{oc}) values in PSC devices. In addition, the highest HOMO and relatively lowest LUMO energy levels were found in the PTDzTV film among all of the polymers, suggesting that the π-conjugation between TDz and the thienylene vinylene units is better than the other combination due to the improved orbital mixing between the donor and acceptor units. The other polymers showed similar E_g^{opt} values, despite their different HOMO energy levels, which may indicate the spatial isolation of HOMOs and LUMOs in their main chain.

Table 1 Polymerization results and thermal properties

Polymers	M_n (kg mol^{-1})[a]	$Đ$[a]	$T_{d5\%}$ (°C)[b]	T_m (°C)[c]	T_c (°C)[c]
PTDzTh	32.9	1.77	406	185	138
PTDzSe	27.4	1.51	414	90	N.D.
PTDzTT	17.8	2.10	397	177	N.D.
PTDzBTh	20.1	1.78	402	185	185
PTDzTV	26.6	1.64	392	154	128

Abbreviations: $Đ$, dispersity; M_n, number average of molecular weights; N.D.: not detected; PTDzBTh, 3,3'-didodecyl-2,2'-bithiophene; PTDzSe, selenophene; PTDzTh, thiophene; PTDzTT, thieno[3,4-*b*]thiophene; PTDzTV, (*E*)-1,2-di-(3-dodecylthiophene)vinylene; SEC, size exclusion chromatography; T_c: crystallization temperature; $T_{d5\%}$: 5 wt% weight loss temperature;TDz, 1,3,4-thiadiazole; TG, thermogravimetry. T_m: melting point.
[a]M_n and $Đ$ were determined by SEC using polystyrene standards in $CHCl_3$.
[b]The 5% weight loss temperatures under nitrogen atmosphere analyzed by TG/DTA measurement.
[c]The T_m and T_c values were determined by DSC measurement.

Crystalline structure

The PSC performance is strongly influenced by the microstructure of the polymer in the photoactive layer, such as the orientation, π-π stacking distance, and crystallinity, among others.[27–31] To investigate these factors, GIWAXS measurements were performed for the pristine

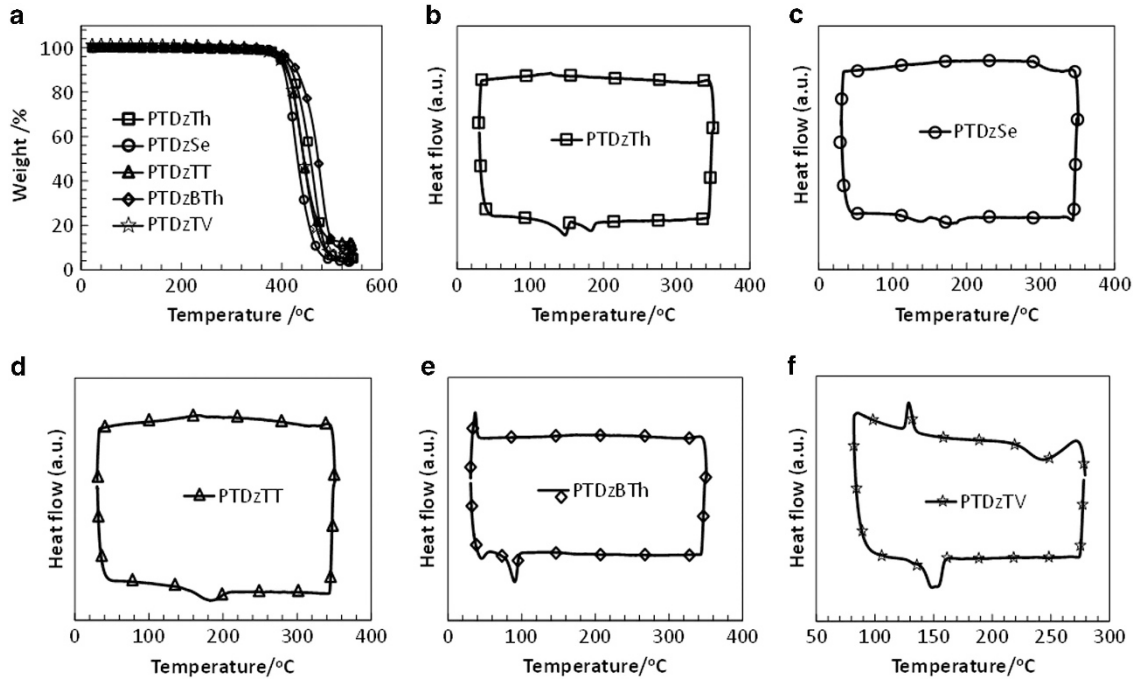

Figure 2 (**a**) TGA curves and (**b**–**f**) DSC charts of TDz-containing polymers.

polymer films, and the obtained two-dimensional GIWAXS images are shown in Figure 5. In particular, π-conjugated polymers exhibit two types of scattering peaks; one peak is attributed to the lamellar spacing distance, which appears in a low q region ($q = 1$–$3\ \mathrm{nm}^{-1}$), and the other peak appears in a high q region ($q = 15$–$18\ \mathrm{nm}^{-1}$), corresponding to the π-π stacking distance. Because the scattering data in the high q_z region is incorrect due to the distortion, we investigated the orientation of the polymer backbone from the lamellar spacing peaks.[31–33] In Figure 6, the scattering intensity in a low q region is plotted as a function of the azimuth angle (ϕ). In this figure, the in-plane and out-of-plane profiles correspond to $\phi = 0°$ and 90°, respectively. Note that the total reflection of light partially overlaps the scattering peak around $\phi = 90°$. Although the pristine films of PTDzBTh and PTDzTV exhibit no scattering peaks in the azimuth profile, PTDzTh and PTDzSe show broad scattering peaks in a low ϕ region, suggesting that the lamellar direction is parallel to the substrate (in-plane direction). Thus, assuming that the polymers form a typical π-stacked lamellar structure, the results indicate that their crystalline structure has a face-on rich orientation. However, a highly oriented edge-on crystalline structure was found in the pristine PTDzTT films. The difference in the orientation may be related to the polymer solubility in the cast solvent, $CHCl_3$, in which highly soluble polymers (PTDzTh and PTDzSe) prefer to form face-on rich crystalline domains, and poorly soluble polymers (PTDzTT) tend to pack

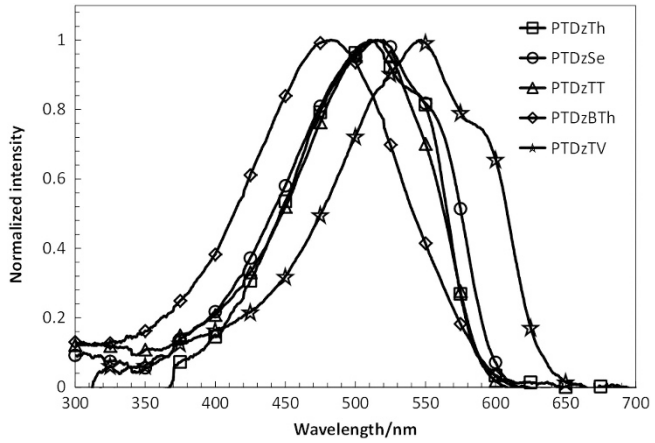

Figure 3 UV–visible spectra of the as-cast polymer films on the quartz substrate.

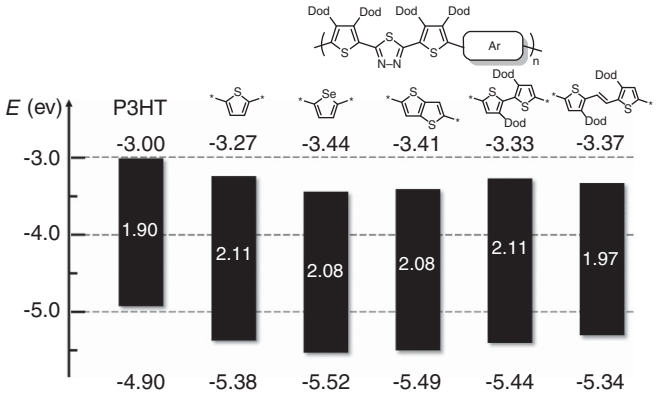

Figure 4 Energy diagrams of rrP3HT and TDz-containing polymers.

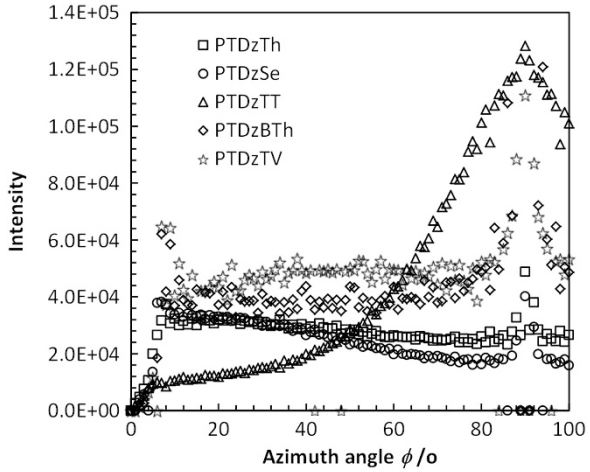

Figure 6 Azimuth plots of the lamellar spacing peaks for the pristine films.

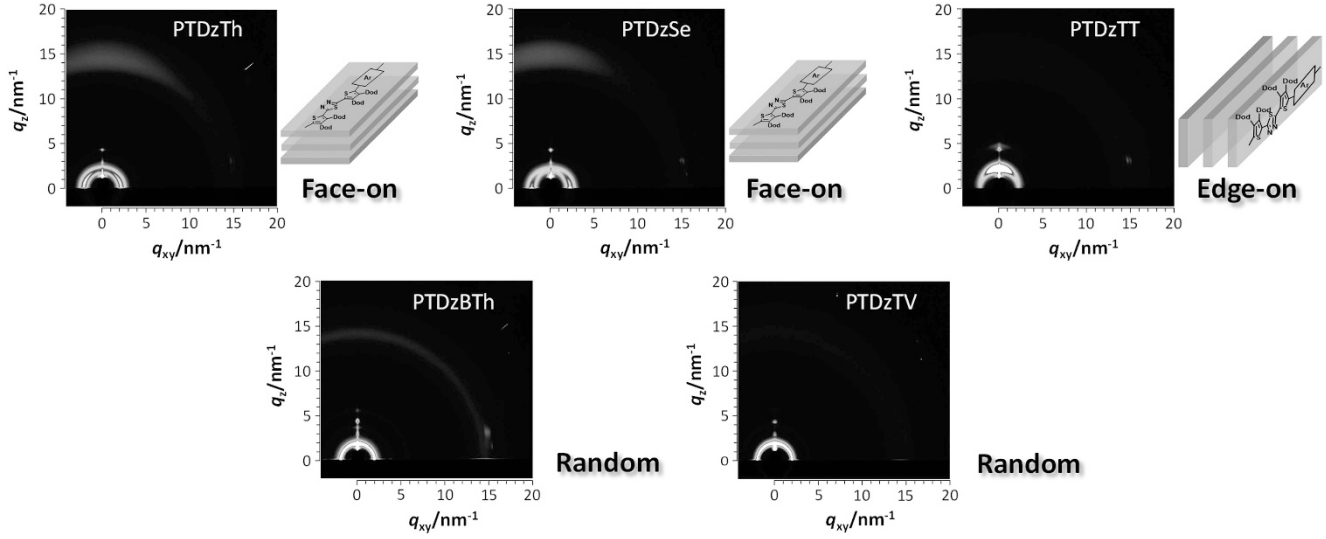

Figure 5 Two-dimensional GIWAXS images of as-cast pristine polymer films.

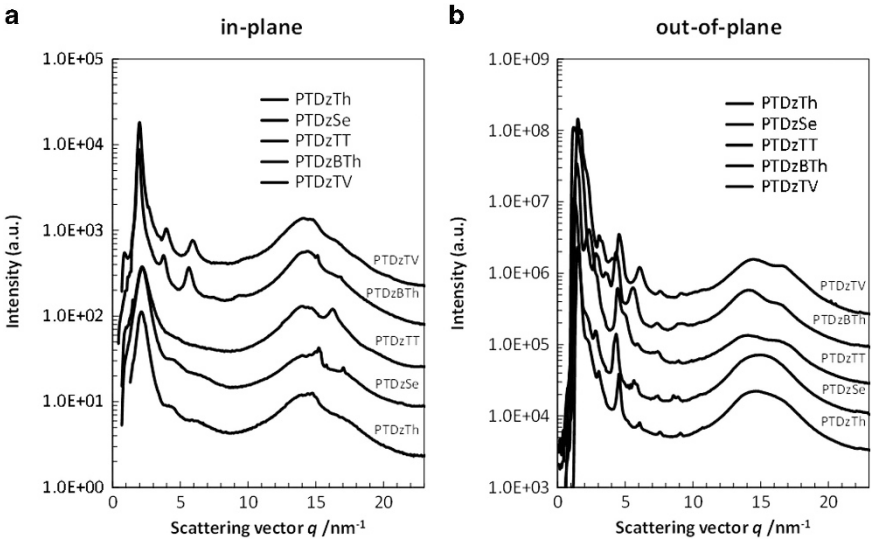

Figure 7 One-dimensional GIWAXS profiles of the pristine polymer films in the (**a**) in-plane and (**b**) out-of-plane direction.

Table 2 Structural parameters based on GIWAXS measurement

		Lamellar spacing		*$\pi-\pi$ Stacking*	
Polymer	*Orientation*	d_{lam} *(nm)*	L_{lam} *(nm)*[a]	$d_{\pi-\pi}$ *(nm)*	$L_{\pi-\pi}$ *(nm)*[a]
PTDzTh	Face-on	2.92	7.74	0.395	1.84
PTDzSe	Face-on	2.85	7.42	0.402	1.91
PTDzTT	Edge-on	2.74	10.2	0.386	5.12
PTDzBTh	Random	3.26	21.4	0.378	3.57
PTDzTV	Random	3.14	22.3	0.373	2.94

Abbreviations: FWHM: full width of half maximum; GIWAXS, grazing incident wide-angle scattering; $d_{\pi-\pi}$, $\pi-\pi$ stacking distance; d_{lam}: lamellar spacing; L_{lam}, correlation length of lamellar spacing; $L_{\pi-\pi}$: correlation length of $\pi-\pi$ stacking distance; PTDzBTh, 3,3′-didodecyl-2,2′-bithiophene; PTDzSe, selenophene; PTDzTh, thiophene; PTDzTT, thieno[3,4-*b*]thiophene; PTDzTV, (*E*)-1,2-di-(3-dodecylthiophene)vinylene.
[a]The correlation lengths were calculated according to the following equation; $L_x = 2\pi/FWHM_x$ (x = lam or $\pi-\pi$).

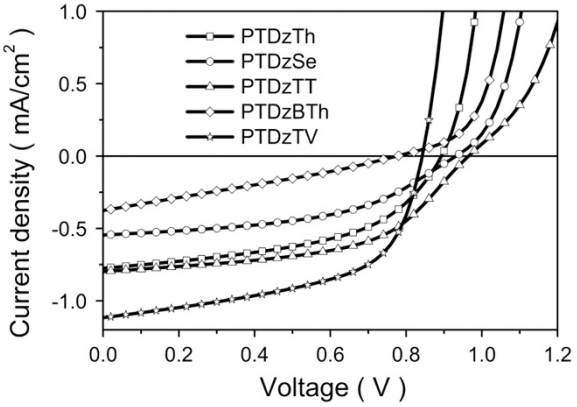

Figure 8 *J-V* characteristics of the devices (ITO/PEDOT:PSS/Polymer:$PC_{71}BM$/Ca/Al) with different donors under 100 mW cm^{-2} illumination of an AM 1.5G solar spectrum.

Table 3 The PSC performance of ITO/PEDOT:PSS/polymer:PC_{71}BM/Ca/Al

Polymer	V_{oc} *(V)*	J_{sc} *(mAcm^{-2})*	*FF*	*PCE (%)*
PTDzTh	0.893	0.775	0.505	0.349
PTDzSe	0.932	0.546	0.482	0.245
PTDzTT	0.965	0.798	0.535	0.412
PTDzBTh	0.776	0.377	0.273	0.080
PTDzTV	0.843	1.120	0.562	0.529

Abbreviations: *FF*, fill factor; J_{sc}, short-circuit current density; PCE, power conversion efficiency; PSC, polymer solar cell; PTDzBTh, 3,3'-didodecyl-2,2'-bithiophene; PTDzSe, selenophene; PTDzTh, thiophene; PTDzTT, thieno[3,4-*b*]thiophene; PTDzTV, (*E*)-1,2-di-(3-dodecylthiophene) vinylene; V_{oc}, open-circuit voltage.

in an edge-on orientation. Similar results were reported for diketopyrrolopyrrole-based polymers by Zhang *et al.*;[34] hence, the same phenomenon most likely occurred in the TDz-based polymers.

The in-plane and out-of-plane profiles are shown in Figure 7, and structural parameters such as the distances of lamellar spacing and π-π stacking (d_{lam}, $d_{\pi-\pi}$), with their correlation length (L_{lam}, $L_{\pi-\pi}$) are summarized in Table 2. All of the polymers exhibit weak and broad scattering peaks in both of the pristine films, and especially, PTDzTh and PTDzSe do not show the higher order of scattering peaks. Therefore, it can be concluded that these five polymers have relatively low crystallinity in the as-cast pristine films. The d_{lam} values of PTDzBTh (3.26 nm) and PTDzTV (3.14 nm) are nearly twice the size of an extended dodecyl group (1.52 nm),[35] implying that they have little interdigitation in a lamellar spacing direction. PTDzTh and PTDzSe show lower d_{lam} values (2.92, 2.85 nm) with lower L_{lam} values (7.74, 7.42 nm), suggesting that their side chains interdigitate to disturb the π-π stacking of the polymer main chains. For PTDzTh and PTDzSe, significantly large $d_{\pi-\pi}$ values (0.395, 0.402 nm) with low $L_{\pi-\pi}$ values (1.84, 1.91 nm) are found. PTDzTT also shows the smallest d_{lam} value (2.74 nm), and the L_{lam} value is relatively high (10.2 nm) among the polymers. The steric hindrance caused by the interdigitation appears to be small, which is supported by the highest $L_{\pi-\pi}$ value (5.12 nm). Thus, PTDzTT shows a good balance between rigidity of the main chain and solubility influenced by the side chains; thus, a highly crystalline order appears in the π-π stacking direction.

PSC performance

To investigate the PSC performance of the synthesized polymers, the PSC devices were fabricated with the standard architecture of glass/

ITO/PEDOT:PSS/polymer:$PC_{71}BM$/Ca/Al. The *J-V* characteristics of the PSCs are shown in Figure 8, and their parameters are summarized in Table 3. Most of the devices showed high V_{oc} values and moderate *FF* values, except for those of PTDzBTh, whose low performance was most likely caused by the low film quality. The V_{oc} values have a tendency to increase as the HOMO energy levels decrease; thus, the lowest HOMO level of the PTDzTT afforded the highest V_{oc} of 0.965 V among the polymers. The J_{sc} values were affected by the E_g^{opt} values and the crystalline nature of the polymers. Comparing PTDzTh, PTDzSe and PTDzTT whose E_g^{opt} values are nearly the same, the narrower $d_{\pi\text{-}\pi}$ and higher $L_{\pi\text{-}\pi}$ values provided slightly improved J_{sc} and *FF*. Therefore, PTDzTT afforded the second highest PCE of 0.412% among the polymers. However, the lowest E_g^{opt} polymer, PTDzTV, yielded a substantially higher J_{sc} value of 1.12 $mAcm^{-2}$ than that of the highly crystalline PTDzTT (0.798 $mAcm^{-2}$). Therefore, it can be concluded that the light absorption behavior of the polymers strongly affects the J_{sc} values, and the highly crystalline structure slightly improves the J_{sc} and *FF* values. However, the TDz polymers containing *n*-dodecyl side chains showed substantially lower performances than that of **P1** having *n*-hexyl side chains, especially in J_{sc}s, and lower shunt resistances, which were suggested by the shallow slopes of the *J-V* curves under the open-circuit condition. We believe that there are difficulties in the charge separation and charge collection processes. Our polymers have substantially longer side chains around the compact acceptor unit than **P1**, so that the $PC_{71}BM$ molecules could not approach the TDz units. Therefore, the charge preparation may be difficult due to the unsuitable intermolecular arrangement.[36] In addition, researchers reported that compared with the polymers with branched side chains, those with linear side chains provide higher non-geminate and geminate recombination rates[37] and can form aggregates with energetically unfavorable states for the charge dissociation.[38] Therefore, we speculate that the replacement of the linear side chains placed around the acceptor unit with the branched side chains placed around the donor unit would improve the J_{sc} and shunt resistance.

CONCLUSION

Novel TDz-based conjugated polymers were synthesized, and their thermal/optoelectronic properties and polymer crystalline structures were investigated. The polymers show moderate molecular weights ($M_n = 17.8$–$32.9\ kg\ mol^{-1}$) and sufficient thermal stability ($T_{d5\%} \sim 400$ °C) for PSC fabrication. All of the polymers exhibit deeper HOMO energy levels (< -5.2 eV) compared with regioregular poly(3-hexylthiophene) due to the electron deficiency of the TDz units. In addition, PTDzTV shows the most extended absorption wavelength ($\lambda_{onset} = 629$ nm) among the polymers due to the improved conjugation length. GIWAXS measurements revealed that PTDzTT shows the highest ordered crystalline structure in the π-π stacking direction due to a good balance between rigidity and solubility. PSCs using TDz-based polymers were fabricated to investigate the photovoltaic performance, and high V_{oc} values up to 0.965 V were achieved because of the deep HOMO energy levels.

ACKNOWLEDGEMENTS

This study was supported by the Japan Science and Technology Agency (JST), PRESTO program (JY 220176). The authors also thank the Japan Society for the Promotion of Science for the partial financial support by KAKENHI (#24655097). SF and SM thank Innovative Flex Course for Frontier Organic Material Systems (iFront) at Yamagata University for their financial support. GIWAXS experiments were performed at the BL46XU of SPring-8 with the approval of the Japan Synchrotron Radiation Research Institute (JASRI; Proposal No. 2014B1590). We thank Professor Itaru Osaka (RIKEN) for conducting the GIWAXS experiments.

1 Yook, K. S. & Lee, J. Y. Small molecule host materials for solution processed phosphorescent organic light-emitting diode. *Adv. Mater.* **26**, 4218–4233 (2014).
2 Allard, S., Forster, M., Souharce, B., Thiem, H. & Scherf, U. Organic semiconductors for solution-processable field-effect transistors (OFETs). *Angew. Chem. Int. Ed. Engl.* **47**, 4070–4098 (2008).
3 Krebs, F. C., Espinosa, N., Hosel, M., Sondergaard, R. R. & Jørgensen, M. 25th Anniversary article: rise to power – OPV-based solar parks. *Adv. Mater.* **26**, 29–39 (2014).
4 Brabec, C. J., Gowrisanker, S., Halls, J. J. M., Laird, D., Jia, S. & Williams, S. P. Polymer–fullerene bulk-heterojunction solar cells. *Adv. Mater.* **22**, 3839–3856 (2010).
5 Li, G., Shrotriya, V., Huang, J., Yao, Y., Moriarty, T., Emery, K. & Yang, Y. High-efficiency solution processable polymer photovoltaic cells by self-organization of polymer blends. *Nat. Mater.* **4**, 864–868 (2005).
6 Yang, X., Loos, J., Veenstra, S. C., Verhees, W. J. H., Wienk, M. M., Kroon, J. M., Michels, M. A. J. & Janssen, R. A. J. Nanoscale morphology of high-performance polymer solar cells. *Nano Lett.* **5**, 579–583 (2005).
7 Dang, M. T., Hirsch, L. & Wantz, G. P3HT:PCBM, best seller in polymer photovoltaic research. *Adv. Mater.* **23**, 3597–3602 (2011).
8 You, J., Dou, L., Yoshimura, K., Kato, T., Ohya, K., Moriarty, T., Emery, K., Chen, C. C., Gao, J., Li, G. & Yang, Y. A polymer tandem solar cell with 10.6% power conversion efficiency. *Nat. Commun.* **4**, 1446–1456 (2013).
9 Cheng, Y. J., Yang, S. H. & Hsu, C. S. Synthesis of conjugated polymers for organic solar cell applications. *Chem. Rev.* **109**, 5868–5923 (2009).
10 Zhou, H., Yang, L. & You, W. Rational design of high performance conjugated polymers for organic solar cells. *Macromolecules* **45**, 607–632 (2012).
11 Guo, X., Baumgarten, M. & Mullen, K. Designing π-conjugated polymers for organic electronics. *Prog. Polym. Sci.* **38**, 1832–1908 (2013).
12 Scharber, M. C., Muhlbacher, D., Koppe, M., Denk, P., Waldauf, C., Heeger, A. J. & Brabec, C. J. Design rules for donors in bulk-heterojunction solar cells—towards 10% energy-conversion efficiency. *Adv. Mater.* **18**, 789–794 (2006).
13 Yasuda, T., Imase, T., Nakamura, Y. & Yamamoto, T. New alternative donor-acceptor arranged poly(aryleneethynylene)s and their related compounds composed of five-membered electron-accepting 1,3,4-thiadiazole, 1,2,4-triazole, or 3,4-dinitrothiophene units: synthesis, packing structure, and optical properties. *Macromolecules* **38**, 4687–4697 (2005).
14 Pang, H., Skabara, P. J., Crouch, D. J., Duffy, W., Heeney, M., McCulloch, I., Coles, S. J., Horton, P. N. & Hursthouse, M. B. Structural and electronic effects of 1,3,4-thiadiazole units incorporated into polythiophene chains. *Macromolecules* **40**, 6585–6593 (2007).
15 Patil, P. S., Haram, N. S., Pal, R. R., Periasamy, N., Wadgaonkar, P. P. & Salunkhe, M. M. Synthesis, spectroscopy, and electrochemical investigation of new conjugated polymers containing thiophene and 1,3,4-thiadiazole in the main chain. *J. Appl. Polym. Sci.* **125**, 1882–1889 (2012).
16 Umeyama, T., Douvogianni, E. & Imahori, H. Synthesis and photovoltaic properties of conjugated polymer based on 1,3,4-thiadiazole unit. *Chem. Lett.* **41**, 354–356 (2012).
17 Higashihara, T., Wu, H. C., Mizobe, T., Lu, C., Ueda, M. & Chen, W. C. Synthesis of thiophene-based π-conjugated polymers containing oxadiazole or thiadiazole moieties and their application to organic photovoltaics. *Macromolecules* **45**, 9046–9055 (2012).
18 Higashihara, T., Mizobe, T., Lu, C., Chen, W. C. & Ueda, M. Synthesis of new thiadiazole-containing polythiophene derivatives and their application to organic solar cells. *J. Photopolym. Sci. Technol.* **26**, 185–191 (2013).
19 Fukuta, S., Koganezawa, T., Tokita, M., Kawauchi, S., Mori, H., Ueda, M. & Higashihara, T. "Face-on" oriented π-conjugated polymers containing 1,3,4-thiadiazole moiety investigated with synchrotron GIXS measurements: relationship between morphology and PSC performance. *J. Photopolym. Sci. Technol.* **27**, 351–356 (2014).
20 Mei, J. & Bao, Z. Side chain engineering in solution-processable conjugated polymers. *Chem. Mater.* **26**, 604–615 (2014).
21 Guo, Z., Lee, D. Y., Liu, Y., Sun, F. Y., Sliwinski, A., Gao, H. F., Burns, P. C., Huang, L. B. & Luo, T. F. Tuning the thermal conductivity of solar cell polymers through side chain engineering. *Phys. Chem. Chem. Phys.* **16**, 7764–7771 (2014).
22 Ko, S., Verploegen, E., Hong, S., Mondal, R., Hoke, E. T., Toney, M. F., McGehee, M. D. & Bao, Z. 3,4-Disubstituted polyalkylthiophenes for high-performance thin-film transistors and photovoltaics. *J. Am. Chem. Soc.* **133**, 16722–16725 (2011).
23 Haid, S., Mishra, A., Weil, M., Uhrich, C., Pfeiffer, M. & Bauerle, P. Synthesis and structure–property correlations of dicyanovinyl-substituted oligoselenophenes and their application in organic solar cells. *Adv. Funct. Mater.* **22**, 4322–4333 (2012).
24 Zhang, G., Fu, Y., Xie, Z. & Zhang, Q. Synthesis of low bandgap polymer based on 3,6-dithien-2-yl-2,5-dialkylpyrrolo[3,4-c]pyrrole-1,4-dione for photovoltaic applications. *Sol. Energy Mater. Sol. Cells* **95**, 1168–1173 (2011).
25 Shi, Q., Fan, H., Liu, Y., Chen, J., Shuai, Z., Hu, W., Li, Y. & Zhan, X. Thiazolothiazole-containing polythiophenes with low HOMO level and high hole mobility for polymer solar cells. *J. Polym. Sci. Part A Polym. Chem* **49**, 4875–4885 (2011).
26 Kim, D. Y., Kim, J., Lim, B., Baeg, K. J. & Yu, B. K. Polymer containing thiophene unit and thienylenevinylene unit, and organic field effect transistor and organic solar cell containing the polymer. US 8466239 B2.

27 Noriega, R., Rivnay, J., Vandewal, K., Koch, F. P. V., Stingelin, N., Smith, P., Toney, M. F. & Salleo, A. A general relationship between disorder, aggregation and charge transport in conjugated polymers. *Nat. Mater.* **12**, 1038–1044 (2013).
28 Rogers, J. T., Schmidt, K., Toney, M. F., Kramer, E. J. & Bazan, G. C. Structural order in bulk heterojunction films prepared with solvent additives. *Adv. Mater.* **23**, 2284–2288 (2011).
29 Yiu, A. T., Beaujuge, P. M., Lee, O. P., Woo, C. H., Toney, M. F. & Frechet, J. M. J. Side-chain tunability of furan-containing low-band-gap polymers provides control of structural order in efficient solar cells. *J. Am. Chem. Soc.* **134**, 2180–2185 (2012).
30 Chen, W., Xu, T., He, F., Wang, W., Wang, C., Strzalka, J., Liu, Y., Wen, J., Miller, D. J., Chen, J., Hong, K., Yu, L. & Darling, S. B. Hierarchical nanomorphologies promote exciton dissociation in polymer/fullerene bulk heterojunction solar cells. *Nano Lett.* **11**, 3707–3713 (2011).
31 Osaka, I., Saito, M., Koganezawa, T. & Takimiya, K. Thiophene–thiazolothiazole copolymers: significant impact of side chain composition on backbone orientation and solar cell performances. *Adv. Mater.* **26**, 331–338 (2014).
32 Kim, G., Kang, S. J., Dutta, G. K., Han, Y. K., Shin, T. J., Noh, Y. Y. & Yang, C. A thienoisoindigo-naphthalene polymer with ultrahigh mobility of 14.4 cm2/Vs that substantially exceeds benchmark values for amorphous silicon semiconductors. *J. Am. Chem. Soc.* **136**, 9477–9483 (2014).
33 Rivnay, J., Mannsfeld, S. C. B., Miller, C. E., Salleo, A. & Toney, M. F. Quantitative determination of organic semiconductor microstructure from the molecular to device scale. *Chem. Rev.* **112**, 5488–5519 (2012).
34 Zhang, X., Richter, L. J., DeLongchamp, D. M., Kline, R. J., Hammond, M. R., McCulloch, I., Heeney, M., Ashraf, R. S., Smith, J. N., Anthopoulos, T. D., Schroeder, B., Geerts, Y. H., Fischer, D. A. & Toney, M. F. Molecular packing of high-mobility diketopyrrolo-pyrrole polymer semiconductors with branched alkyl side chains. *J. Am. Chem. Soc.* **133**, 15073–15084 (2011).
35 Pan, H., Wu, Y., Li, Y., Liu, P., Ong, B. S., Zhu, S. & Xu, G. Benzodithiophene copolymer—a low-temperature, solution-processed high-performance semiconductor for thin-film transistors. *Adv. Funct. Mater.* **17**, 3574–3579 (2007).
36 Graham, K. R., Cabanetos, C., Jahnke, J. P., Idso, M. N., Labban, A. E., Ngongang, N. G. O., Heumueller, T., Vandewal, K., Salleo, A., Chmelka, B. F., Amassian, A., Beaujuge, P. M. & McGehee, M. D. Importance of the donor:fullerene Intermolecular arrangement for high-efficiency organic photovoltaics. *J. Am. Chem. Soc.* **136**, 9608–9618 (2014).
37 Smith, C. D., Howard, I. A., Cabanetos, C., Labban, A. E., Beaujuge, P. M. & Laquai, F. Interplay between side chain pattern, polymer aggregation, and charge carrier dynamics in PBDTTPD:PCBM bulk-heterojunction solar cells. *Adv. Energy Mater* (e-pub ahead of print 29 January 2015; doi:10.1002/aenm.201401778).
38 Guo, Z., Lee, D., Schaller, R. D., Zuo, X., Lee, B., Luo, T., Gao, H. & Huang, L. Relationship between interchain interaction, exciton delocalization, and charge separation in low-bandgap copolymer blends. *J. Am. Chem. Soc.* **136**, 10024–10032 (2014).